Factor analysis of medical image sequences in MR of head and neck tumors.

A M Zagdanski, R Sigal, J Bosq, J P Bazin, D Vanel and R Di Paola

AJNR Am J Neuroradiol 1994, 15 (7) 1359-1368
http://www.ajnr.org/content/15/7/1359

Factor Analysis of Medical Image Sequences in MR of Head and Neck Tumors

Anne-Marie Zagdanski, Robert Sigal, Jacques Bosq, Jean-Pierre Bazin, Daniel Vanel, and Robert Di Paola

PURPOSE: To evaluate factor analysis of medical image sequences (FAMIS), a means whereby physiologic contrast enhancement kinetics, called *factors*, and their spatial distribution, termed *factor images*, are estimated after acquisition of dynamic MR images. The method is intended to recognize and characterize the different tissue kinetics automatically. **METHODS:** This method was evaluated in a series of 22 patients with head and neck tumors. Eleven patients presented with a previously untreated lesion. Six were examined for tumor recurrence, previously treated by multiple therapies. Five patients had preoperative chemotherapy and underwent MR before and after chemotherapy. In all cases, MR images were correlated with surgical and pathologic data. MR examinations were performed on a 1.5-T unit with static sequences and dynamic sequences acquired after bolus injection of gadolinium and processed by FAMIS. **RESULTS:** FAMIS was able to identify three factors representing contrast-enhancement kinetics and their associated factor images. The neoplastic component was associated with the earlier factor image, F1. Fibrosis and chemotherapy and/or radiation-induced changes were associated with the two later factors, F2 and F3. The limits of this method were highly vascularized tissues whose earlier factor was similar to that of neoplastic tissues (mucosae and salivary glands), patient motion, responsible for artifacts in FAMIS, and lesions of less than 5 mm. **CONCLUSION:** FAMIS of dynamic MR studies was useful for differentiating neoplastic tissue from tissue having undergone changes by chemotherapy and/or radiotherapy, but it did not improve the ability of MR to characterize neoplastic tissues in previously untreated patients.

Index terms: Magnetic resonance, technique; Magnetic resonance, tissue characterization; Head, neoplasms; Neck, neoplasms

AJNR Am J Neuroradiol 15:1359–1368, Aug 1994

Many studies have pointed out the ability of magnetic resonance (MR) imaging to delineate the extension of head and neck tumors. Visualization of deep-seated soft tissues complements the clinical assessment of malignancies. However, MR is unable to establish tissue characterization, and biopsy remains mandatory to obtain the histologic diagnosis (1). Moreover, differentiation between neoplastic and inflammatory tissues may be difficult, particularly in the early months after therapy (2, 3). Recurrent or residual tumor and posttherapy tissue changes may have the same signal intensity.

Factor analysis of medical image sequences (FAMIS) has been used to overcome this inconvenience. In this method, dynamic gadolinium-enhanced MR images are processed for a precise analysis of contrast-enhancement kinetics in different tissues. Its efficiency has been demonstrated in the prediction of the response of osteosarcoma to chemotherapy (4). In this prospective study, we analyze the results of this technique in a series of 22 patients presenting with head and neck neoplasms. MR studies performed in untreated tumors and multimodality-treated tumors were compared in all cases with the resected specimens.

Received June 11, 1993; accepted pending revision August 25; revision received September 14.

From INSERM U66 (A.-M.Z., J.-P.B., R.D.P.), Departments of Radiology (A.-M.Z., R.S., D.V.), and Pathology (J.B.), Institut Gustave Roussy, Villejuif, France.

Address reprint requests to Robert Sigal, MD, PhD, Department of Radiology, Institut Gustave Roussy, F-94805 Villejuif Cedex, France.

AJNR 15:1359–1368, Aug 1994 0195-6108/94/1507–1359

Patients and Methods

Patients

Twenty-two patients, ranging from 19 to 72 years of age (average, 55.3 years) were prospectively studied from February to July 1992. All patients underwent surgery. The primary sites were the oral cavity (18 patients), masticator space (1 patient), nasal fossa (1 patient), and paranasal sinuses (2 patients). The malignant histologic types included 17 squamous cell carcinomas, 1 adenoid cystic carcinoma, and 1 rhabdomyosarcoma. The benign histologic types included 1 inverted papilloma and 2 chronic inflammatory lesions of the maxillary sinuses mimicking tumors.

Eleven patients presented with untreated lesions, and 11 patients had single or multiple treatment at the time of MR. Among the latter, 6 patients presented with recurrent or progressive disease previously treated by multiple modalities (surgery, chemotherapy, and radiation therapy). In all cases, the last treatment was performed 1 to 27 months (mean 7.8 months) before this study. In 3 cases, the last treatment was only surgery, which had been performed, respectively, 1, 2, and 27 months before MR examination. Three cases were treated by surgery, radiation therapy, and/or chemotherapy during a mean period of 36 months. The last treatment in these patients was done 3, 4, and 11 months before MR examination. The 5 other patients underwent preoperative chemotherapy (two to three courses of intravenous cisplatin [cis-diammine-dichloroplatinum] and fluorouracil), which ended 2 to 4 weeks (mean, 22 days) before surgery.

Imaging Procedure

MR studies were done 3 to 25 days before surgery (average, 11.4 days). The five patients who had preoperative chemotherapy underwent MR examination before and after the chemotherapy. Therefore, a total of 27 MR examinations were analyzed.

MR examinations were performed on a 1.5-T system (Signa, General Electric, Milwaukee, Wis) using a standard head coil.

All the patients were studied before gadolinium injection with a sagittal, axial, and coronal T1-weighted (400–600/12 [repetition time/echo time]) and sagittal or coronal proton density-/T2-weighted (2000/30–100) spin-echo images. A 16- to 18-cm field of view and a 192 × 256-pixel acquisition matrix were used with a 5-mm section thickness and 2.5-mm intersection gap.

Dynamic gadolinium-enhanced MR studies were done after rapid injection (4 mL/s, 0.2 mL/kg) of Gd-DOTA (Dotarem, Guerbet Laboratories, France). A short multisection sequence (300/20, four to six sections) was applied once before injection and 14 times after Gd-DOTA injection, during a period of 7 minutes. The dynamic studies were acquired with a 20-cm field of view, a 128 × 256-pixel acquisition matrix, a 5-mm section thickness, and a 2.5-mm intersection gap. Scan time was 25 seconds with a 3-second pause between two successive acquisitions. The patient was asked to swallow only during the pause. The dynamic studies were acquired either in the coronal or sagittal plane, because the resected specimen were cut in those planes.

After completion of this dynamic sequence, two or three additional T1-weighted sequences, in orthogonal planes, were acquired with the same parameters as those used in the pregadolinium study. Therefore, these sequences and those acquired before gadolinium injection were called *static* MR studies, as opposed to the dynamic gadolinium-enhanced MR studies.

Dynamic MR Processing by Factor Analysis of Medical Image Sequences

Image processing was performed using a VAX 8300 computer system (Digital Equipment Corporation, Maynard, Mass) with image display on a 1024 × 1024-pixel graphic processor Sigmex (Sigmex SA-Apricot, Les Ulis, France). The FAMIS algorithm, written in Fortran 77, analyzes the evolution in time of the signal intensity throughout the image during the dynamic sequence (5, 6). FAMIS estimates the different contrast enhancement kinetics, called *factors*, which are functions of time. The spatial or anatomic distribution of each factor is also displayed on an image, called a *factor image*. In a factor image, the signal intensity varies according to the weight of the factor in each pixel. For a given section level, there are as many factor images as kinetic factors. It is possible to superimpose the different factor images using a true-color scale for each individual factor image.

Histologic Procedure

Dynamic MR studies, processed by FAMIS, and static MR studies were compared with histologic sections obtained at the same level. The resected specimens were cut in the same orientation as that used for the dynamic MR studies (coronal or sagittal planes) by the pathologist in the presence of the radiologist. Once fixed and embedded in paraffin, 5-μm sections were obtained and stained with hematoxylin-eosin-safran. The resected specimens, which comprised bone structures, were previously decalcified.

In 11 untreated patients, the following findings were recorded: size of tumor and its extension in the adjacent soft tissues, tissue changes other than tumor (fibrosis and necrosis), and bone involvement. In the other 11 patients with previously treated tumors, any residual neoplastic components were additionally evaluated according to the UICC TNM classification of malignant tumors (7): R0 indicating no residual tumor; R1, tumor residue only detectable at the microscopic level; and R2, tumor mass detectable by the naked eye on the stained tissue sections.

Results

Twenty-seven MR studies were analysed. In 21 of 27 dynamic studies, three factors were

TABLE 1: Findings on FAMIS with pathologic and MR correlation in 10 untreated patients

Patient	Histologic Findings	Location	FAMIS Data			Static MR Data		
			F1	F2	F3	T1WI	T2WI	Gd-T1WI
1	SCC	Tongue and floor of the mouth	++	+		=	+	+
2	SCC	Tongue	++			=	+	+
3	SCC	Tongue	++	+		=	+	+
4	SCC	Floor of mouth	++	+		=	+	+
5	SCC	Tongue	++	+		=	+	+
6	SCC	Gum	++			=	+	+
7	SCC	Tongue	++		+	=	+	+
8	SCC	Floor of mouth	++	+		=	+	+
9	SCC	Tongue + floor of the mouth	++	+	+	=	+	+
10	Fibrosis/mucosa	Maxillary sinus	+		++	=	=	+

Note.—SCC indicates squamous cell carcinoma; T1WI, T1-weighted image; T2WI, T2-weighted image; Gd-T1WI, T1-weighted image with gadolinium injection. On FAMIS, + indicates visibility of the factor; ++, marked visibility of the factor. On static MR, = denotes isointensity to muscle; +, hyperintensity.

identified by FAMIS. The first one, called F1, showed an early kinetic pattern with a maximum-intensity peak within the first 2 minutes (average 0.8 minutes) followed by a slow descending slope. The second factor, called F2, showed a delayed kinetic pattern with a slow ascending slope, a maximum intensity peak within the first 2 to 3 minutes (average 2.3 minutes), and a descending slope. The last factor, named F3, had a gradual growing kinetic pattern which finally plateaued usually after the sixth minute. Figure 1B is a fair illustration of this factor patterns. In 2 of 27 studies, only factors F1 and F3 were extracted. In 4 of 27 studies, factor images, factors, and generally the MR images themselves were deteriorated by motion artifacts. Because of significant fluctuations, the factors did not match the curves obtained in the other studies, and the results could not be interpreted. On the factor images, the motion was translated into edged structures mainly visible at the boundaries between regions, with marked differences in signal intensity.

In the 23 of 27 contributing cases, the normal mucosae of the oral cavity and nasal fossa, the salivary glands (sublingual and submandibulary glands), the lingual tonsil, and the intraorbital muscles were associated with factor F1. The muscles of the infratemporal fossa and oral cavity corresponded to factors F2 and F3. No enhancement was detected in fatty tissues.

A comparison between presurgical FAMIS data and pathologic findings was possible in 19 of 22 cases (10 untreated and 9 previously treated patients).

In nine untreated patients (patients 1 through 9, Table 1), the earlier factor, F1, was predominant in the tumor area (Figs 1 and 3) and was found either alone (two of nine cases) or with factor F2 (six of nine cases) or F3 (one case). Necrosis, found in two cases, corresponded to a void signal. At histologic analysis, there was no significant fibrotic component in these patients. On static T1-weighted sequences, these lesions had a low signal intensity similar to the muscle signal intensity. On the T2-weighted images, the lesions had a varying degree of high signal intensity, which allowed them to be differentiated from adjacent muscles. All the lesions enhanced diffusely on Gd-DOTA T1-weighted images. In the remaining untreated patient (patient 10), with a chronic inflammatory lesion of the maxillary sinus mimicking a tumor, the fibrotic mass was predominantly associated with F3, whereas both the normal and the inflammatory mucosae were associated with F1.

Among nine previously treated patients (Table 2), four had both prechemotherapy and postchemotherapy MR studies (patients 11 to 14). In these four patients, a comparison between FAMIS images obtained before and after chemotherapy showed that factor F1 associated with the tumor was stable (one case), reduced in size (one case), or had disappeared (two cases). Foci of residual tumor were observed by the pathologist in all cases (Fig 4), either microscopically (R1 pattern in two cases) or on gross specimen (R2 pattern in two cases). FAMIS seems to be unable to identify tumors smaller than 5 mm. In all four cases, pathologic

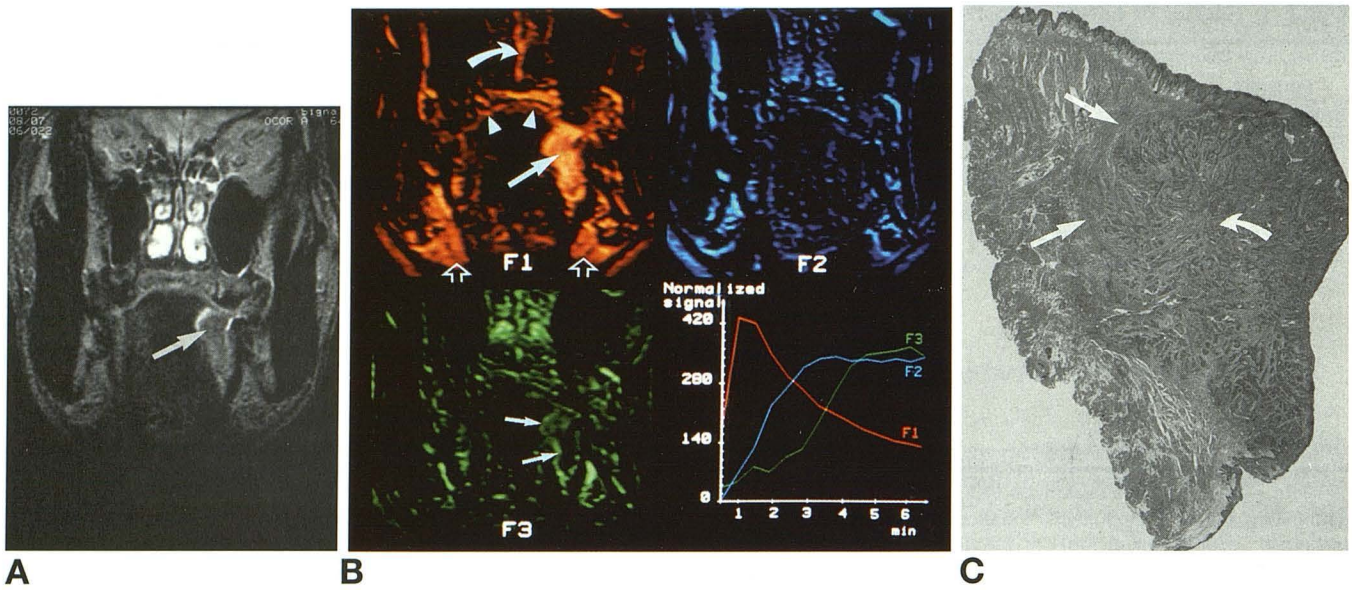

Fig 1. Squamous cell carcinoma of the tongue (patient 7). No previous treatment.

A, Coronal T2-weighted image. The tumor is depicted as a high-signal-intensity area (*arrow*).

B, FAMIS images and factors. The F1 factor image shows the tumor (*arrow*) and hypervascularized structures: lingual mucosa (*arrowheads*), nasal septum (*curved arrow*), and submandibulary glands (*open arrows*). The tumor does not appear on the F2 factor image. A peripheral rim is seen around the tumor (*arrows*) on the F3 factor image. The *curves* show the three contrast-enhancement kinetics. The origin of the axis is at 28 seconds; this explains why the curves do not start at the zero value.

C, Histologic section shows the lesion composed of central squamous cells (*curved arrow*) with a pseudocapsule of compressed muscle tissue (*arrows*) corresponding to the peripheral rim seen on factor F3 image (hematoxylin and eosin, ×20).

examinations disclosed fibrotic changes associated with factors F2 and F3. On static T1-weighted images, residual tumor and fibrosis had a low signal and enhanced diffusely after gadolinium injection. In three cases, fibrosis had a low signal on T2-weighted images. When there was an absence of regression (one case), tumor had a high signal intensity in T2-weighted images.

The five other patients presented with previously treated neoplasms (patients 15 to 19). After a single operation (three cases) or 11 months after the last treatment (one case), posttherapeutic fibrosis, corresponding to the factors F2 and F3 on factor images, was found at histologic examination in two specimens. As noted in the untreated patients, factor F1 was indicative of the tumor component. However, in one case, a tumor smaller than 5 mm was not detected (patient 15). The tumor component, on the static MR, had the same features as in cases of untreated tumors, and the small amount of fibrosis could not be differentiated from the tumor. The last case (patient 19, Fig 2) presented with multiple relapses; his last treatment was chemotherapy 3 months before MR study. The histologic examination revealed a tumor associated with marked fibrosis. In FAMIS factor images, tumor and fibrosis were clearly separated, with the tumor corresponding to factor F1 and the fibrosis to factors F2 and F3. On static MR, tumor and fibrosis had the same signal intensity in all the sequences. They showed a low signal on T1-weighted images, a high signal whose degree of intensity varied on T2-weighted images, with enhancement after gadolinium injection.

Bone involvement was evidenced by histologic examination in four cases and by FAMIS images in only two cases. One case was associated with factor F1 and corresponded to active tumor at histologic analysis, whereas the second case was associated with factors F2 and F3 and corresponded to fibrotic postchemotherapy changes. The other two cases were seen on static MR as low-signal-intensity areas on T1-weighted images. However, they were not seen on FAMIS images because their size was less than 5 mm.

Discussion

Numerous studies during the past decade have reported the utility of MR in the evaluation

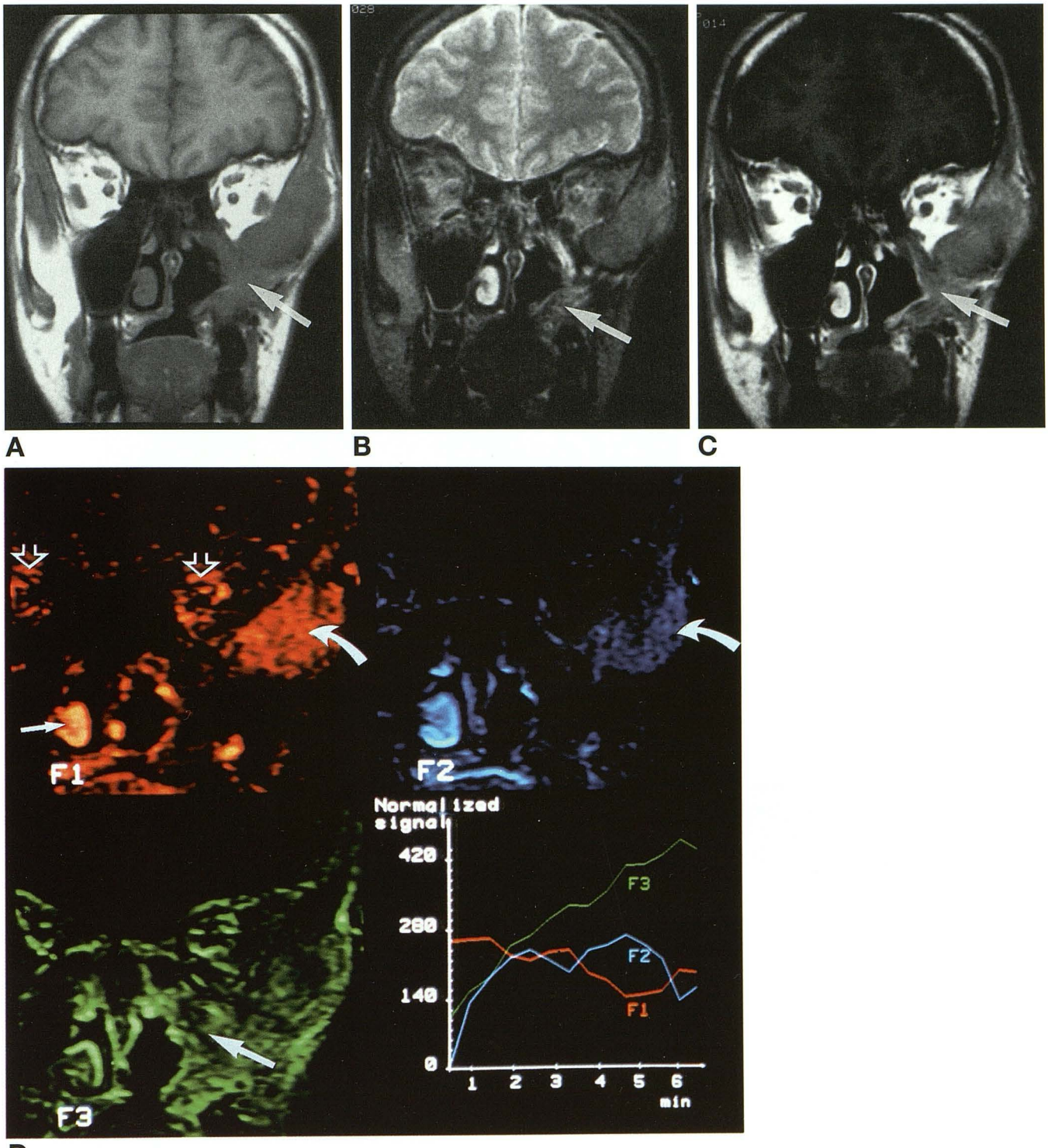

Fig 2. Rhabdomyosarcoma of the masticator space extending along the temporalis muscle (patient 19). Multiple previous therapy.

A, Coronal T1-weighted image.

B, Coronal T2-weighted image.

C, Coronal T1-weighted image after Gd-DOTA injection. The lesion is homogeneous on all sequences; it is not possible to differentiate the tumor from changes induced by therapy, particularly next to the maxillary sinus (*arrow*).

D, FAMIS images and factors. The F1 factor image shows the tumor (*curved arrow*), the extraorbital muscles (*open arrows*), and the inferior right turbinate (*arrow*). The F2 factor image faintly shows the tumor (*curved arrow*). The area next to the maxillary sinus appears on the F3 factor image and corresponds to posttherapeutic fibrosis (*arrow*).

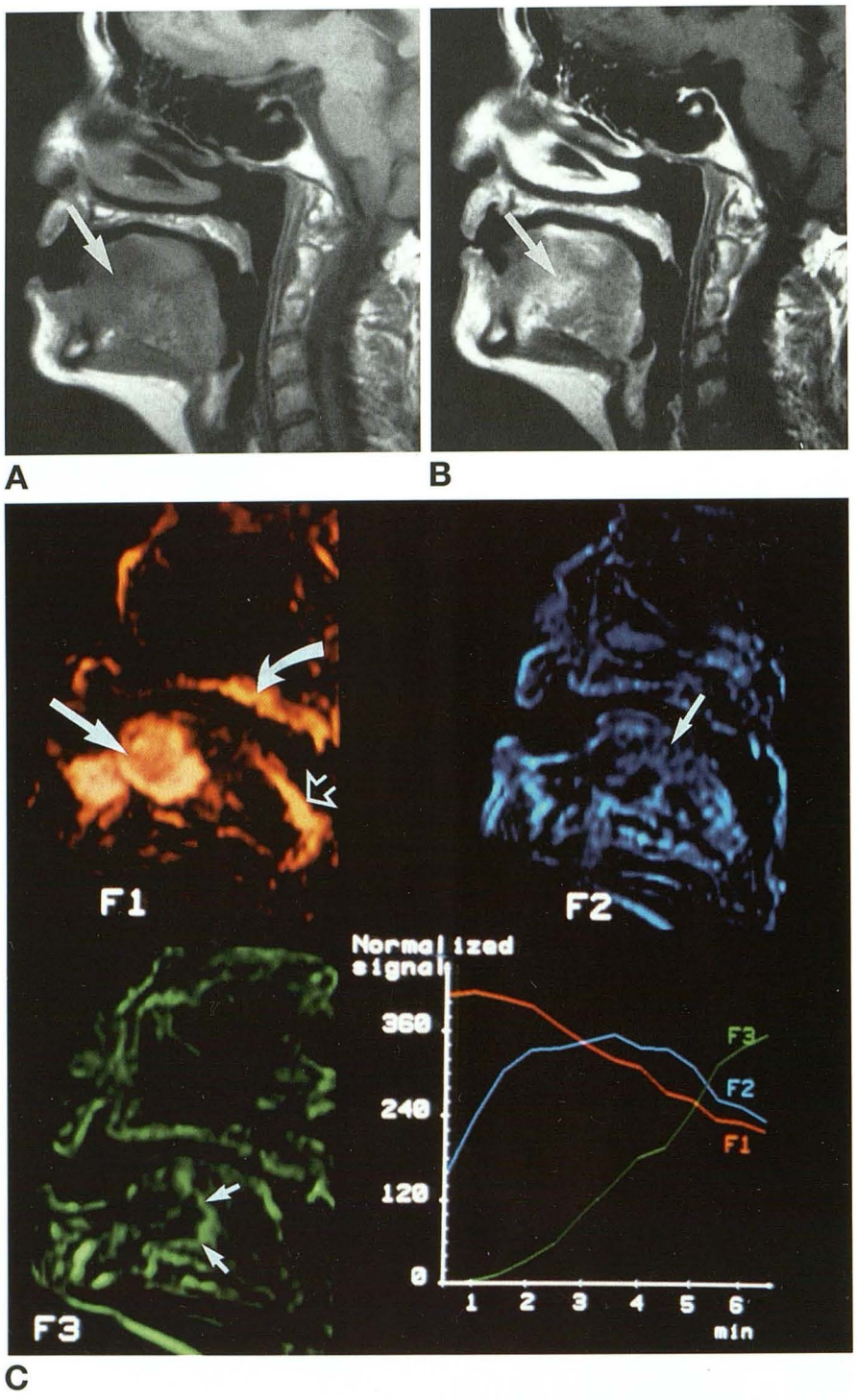

Fig 3. Squamous cell carcinoma of the tongue and floor of the mouth (patient 12). No previous treatment.

A, Sagittal T1-weighted image. The tumor is depicted as a low-signal-intensity area (*arrow*).

B, Sagittal T1-weighted view after Gd-DOTA injection. The tumor enhances with contrast (*arrow*).

C, FAMIS images and factors. The F1 factor image shows the tumor (*arrow*) and hypervascularized structures: palate (*curved arrow*) and lingual tonsil (*open arrow*). The F2 factor image displays normal muscles of the tongue (*arrow*). On the F3 factor image, a peripheral rim is seen around the tumor (*arrows*), as in Figure 1B.

of patients with head and neck disease. MR provides useful information on extension in soft tissue and differentiation between tumor and inflammatory tissues, in particular in the sinonasal area (8). Although MR may help assess the aggressiveness of malignant lesions (9), it cannot accurately establish the histologic type. This shortfall underscores the need for a biopsy to obtain an accurate histologic diagnosis (1).

The limitations of MR in tissue characterization are even greater in previously treated patients (2). Previous therapy, in particular radiation therapy and chemotherapy, is responsible for stromal reaction, in particular fibrosis and

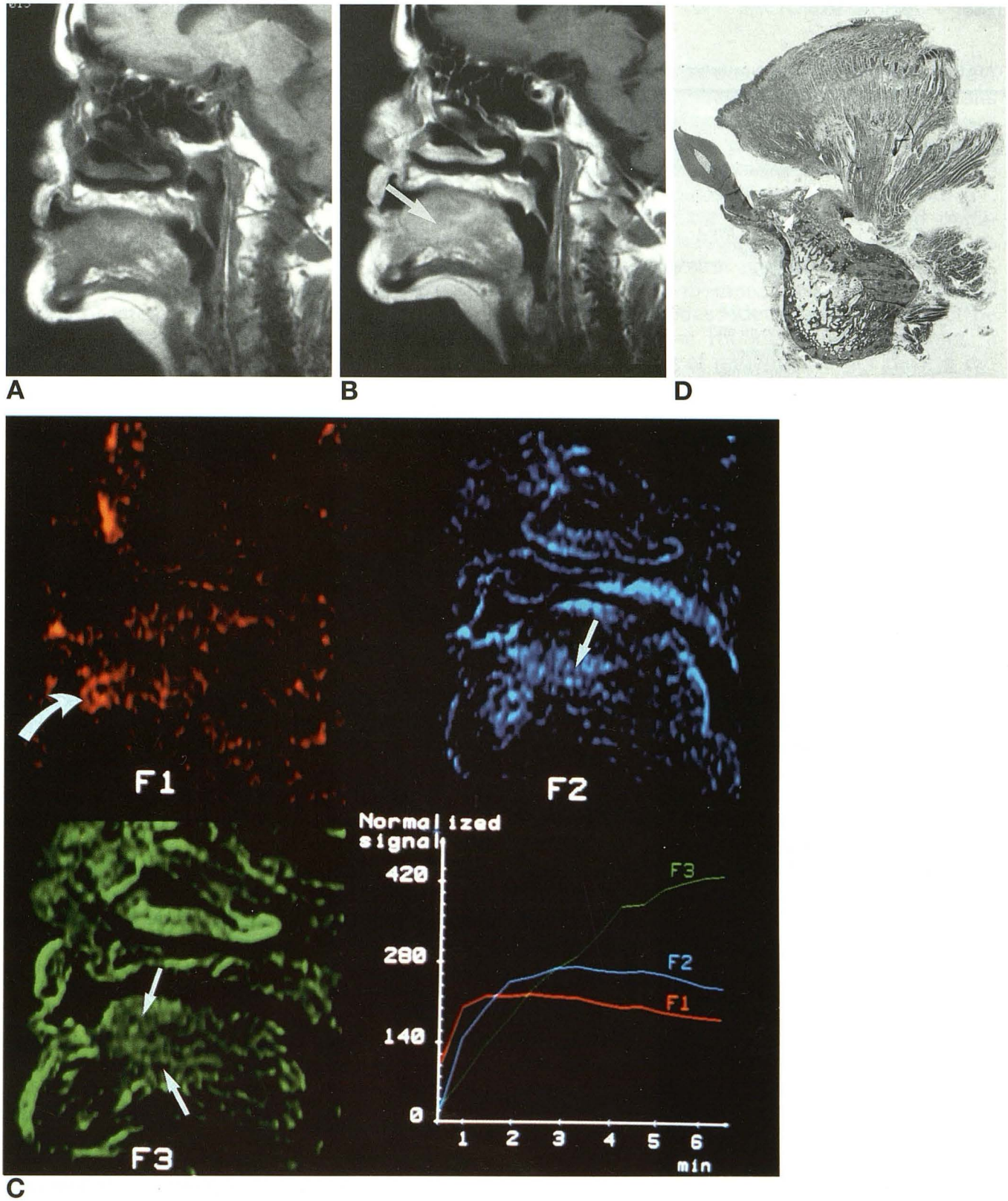

Fig 4. Same patient as Figure 3. Squamous cell carcinoma of the tongue and floor of the mouth. Examination performed 14 days after completion of chemotherapy.

A, Sagittal T1-weighted image.

B, Sagittal T1-weighted view after Gd-DOTA injection. The floor of the mouth and the mobile portion of the tongue enhance after contrast injection (*arrow*). It is not possible to differentiate residual tumor from chemotherapy-induced fibrosis.

C, FAMIS images and factors. The F1 factor image exhibits small tumor foci (*curved arrow*). The F2 and F3 factor images show extensive fibrosis (*arrows*).

D, Histologic section shows small clusters of squamous cells (*arrows*) developed in a large fibrous stromal tissues (hematoxylin and eosin, ×10).

TABLE 2: Findings on FAMIS with pathologic and MR correlation in nine previously treated patients

Patient	Histologic Findings	Location	Previous Treatment	Date of Last Treatment	Histologic Data	FAMIS Data			Static MR Data		
						F1	F2	F3	T1WI	T2WI	Gd-T1WI
11	SCC	Floor of the mouth	Chemotherapy	3 wk	R1 Fibrosis			++	=	=	+
12	SCC	Floor of the mouth and tongue	Chemotherapy	2 wk	R2 Fibrosis	+	++	++	=	=	+
13	SCC	Tongue	Chemotherapy	3 wk	R2 No fibrosis	++		+	=	+	+
14	SCC	Floor of the mouth and tongue	Chemotherapy	3 wk	R1 Fibrosis			++	=	=	+
15	SCC	Floor of the mouth	Surgery	1 mo	R1 Fibrosis			++		not visible	
16	SCC	Floor of the mouth	Surgery	27 mo	R2 Fibrosis	++	+		=	+	+
17	Adenoid cystic carcinoma	Floor of the mouth	Surgery, radiotherapy	11 mo	R2 Fibrosis	++	+	+	=	+	+
18	Inverted papilloma	Nasal fossa	Surgery	2 mo	R2 Fibrosis	++	+	+	=	+	+
19	Rhabdomyo-sarcoma	Infratemporal fossa	Surgery, chemotherapy, radiotherapy	3 mo	R2 Fibrosis	++	+	+ ++	=	+	+

Note.—SCC indicates squamous cell carcinoma; R1, tumor residue detectable only at the microscopic level; R2, tumor residue detected by the naked eye; T1WI, T1-weighted image; T2WI, T2-weighted image; Gd-T1WI, T1-weighted image with gadolinium injection. On FAMIS, +, indicates visibility of the factor; ++, marked visibility of the factor. On static MR, = denotes isointensity to muscle; +, hyperintensity.

chronic inflammatory changes (10). These changes can appear as soon as treatment has been completed and may progress for several months.

At MR, it is difficult to distinguish posttherapeutic tissue changes from recurrent or progressive disease. Several authors have studied the characteristics of fibrosis on MR. Lee and Glazer have defined criteria to characterize fibrosis according to its age (11). Early fibrosis has a high signal intensity on T2-weighted images because it is composed of numerous fibroblasts and vascular endothelial cells, but few collagen fibers, whereas mature fibrosis has a low-signal intensity because its cellularity is poor. The use of paramagnetic contrast agents fails to provide further information because both tumor and early inflammatory changes take contrast (12).

In our study, the results of static MR were consistent with previously published data. The limits of the untreated lesions were clearly delineated and corresponded to the limits of the tumors themselves, because there were essentially no reactive changes in the adjacent soft tissues, as proved histologically. Conversely, in previously treated patients, MR was not always able to differentiate between tumor and fibrosis. On T2-weighted images tumors presented with a high-signal intensity, whereas the signal of fibrosis was variable. Interestingly, in three patients who had chemotherapy just before MR, the fibrosis had a low signal intensity on T2-weighted images. This does not correspond to the expected signal intensity of young fibrosis (11) but is in accordance with the description of postchemotherapy residual masses in Hodgkin disease (13) and malignant bone tumors (12). At histologic analysis, the stromal reaction comprised dense fibrosis associated with a mild inflammatory reaction. The other patients who had received preoperative chemotherapy had heterogeneous high-signal-intensity areas on T2-weighted images. The histologic diagnosis disclosed a persistent tumor (R2) without fibrosis in one case and intense stromal inflammatory changes with residual tumor in the other case.

The evolution of the uptake of gadolinium also has been studied in an attempt to verify the presence of residual tumor after chemotherapy (12). To assess response to preoperative chemotherapy in bone tumors, Erlemann et al used time-intensity curves derived from rapidly acquired, dynamic gadolinium-enhanced MR images (12). This method has proved its efficiency

in showing that nonresponders have similar patterns of signal intensity before and after chemotherapy, whereas the signal intensity decreases after chemotherapy in responders. However, this method is capable of evaluating only average enhancement of the pixels in the selected region of interest and therefore cannot identify tumor nodules in predominantly inflammatory tissues.

FAMIS offers several advantages over the regions-of-interest method. The entire dynamic image is analyzed automatically, thus avoiding operator-dependent selection of regions of interest. Factors and factor images, estimates of enhancement kinetics, and associated spatial distribution are extracted. Moreover, the mathematical model takes into account factor superimposition in the very same voxel, corresponding to a mixture of different tissues, each with its own particular contrast kinetics. This method was first developed in nuclear medicine (5, 6, 14) and then extended to other modalities (15). In MR, it has been used to predict the response of osteosarcoma to chemotherapy (4). As in our study, three factors were described. The early factor was associated with the viable tumor and disappeared in the tumor area in all responders.

In our study, the early factor, F1, consistently signified tumor but also normal highly vascularized tissues, such as mucosae of the nasal fossa and oral cavity, salivary glands, lingual tonsil and intraorbital muscles (16). The late factors, F2 and F3, were associated with the muscles of the infratemporal fossa and the oral cavity and the medullary bone of the mandible, but also with the fibrosis. Because fibrosis was absent in previously untreated patients, FAMIS did not contribute at this stage. Conversely, in patients with previous treatment, FAMIS allowed us to differentiate tumor from posttherapeutic changes. This was particularly useful in patients who had recently (less than 3 months) received radiation therapy and/or chemotherapy, because signal-intensity characteristics of tumor and fibrosis can be misinterpreted on static MR. The present limits of FAMIS are indicated by the false-negative results in three patients, in whom residual tumor smaller than 5 mm was discovered by the pathologist. These limits could be caused by motion artifacts and/or low-enhancement signal in small tumor components. Second, mucosae and salivary glands also corresponded to factor F1. When a tumor was close to such a tissue, it was difficult to determine its extension precisely. In the same way, we can suppose that superficial mucosal lesions might go undetected, although they remain accessible to clinical assessment. The lack of specificity of FAMIS was also evidenced by the fact that all tumors were associated with F1, including one case of benign inverted papilloma. Another drawback of this method was its sensitivity to motion artifacts. This is particularly evident in examinations of the head and neck. In our series, four studies could not be used because of motion artifacts. In fact, a greater number of patients did not have a dynamic study because of significant motion artifact on the precontrast static study. Finally, the acquisition time of the dynamic sequence is short (7 minutes), whereas the time required for FAMIS processing remains relatively long on the VAX 8300 (approximately 30 minutes). This time could be drastically shortened on more recent systems.

For the present, we can merely speculate on the physiologic mechanisms that underlie the factors that are described by FAMIS. Our hypotheses stem from data on the pharmacokinetic properties of gadolinium and knowledge of the histologic structure of tumors, particularly with respect to neovascularization. Nonspecific contrast media are characterized by a lack of tissue selectivity, short plasma half-lives, and simple distribution throughout the extracellular fluid space (17). Neoplastic tumor vessels have specific characteristics demonstrated by comparative angiographic and pathologic studies (18, 19). They are devoid of nonstriated musculature and have similar structures to that of sinusoids and large capillaries. Moreover, in tumor neovascularity, the tapering of normal vessels is missing, and the caliber of vessels fluctuates. An abnormal course and distribution of proximal large arteries, obstructions, and arteriovenous shunts are also found in tumor vessels. This results in the acceleration of blood flow velocity, as demonstrated by Doppler sonography (20). In FAMIS, the early kinetic pattern, F1, is consistent with increased blood-flow velocity in the tumor. However, this pattern is also associated with normal structures, which have a rich vascularity: extraocular muscles (16), salivary glands, and mucosae (21, 22). F2, the delayed kinetic pattern, is associated with structures with less vascular velocity. It is found in the muscles of the oral cavity and infratemporal fossa and in fibrosis. F2 is also

found in the structures associated with factor F1, and in particular, in the tumor itself. This probably stems from the coexistence of normally structured vessels and histologically abnormal vessels. Finally, the kinetic pattern of the later factor F3 is consistent with the free distribution of the Gd-DOTA throughout the extracellular fluid space (23, 24) and therefore is seen in all the vascularized tissues, be they normal or abnormal.

Acknowledgments

We thank Ms Lorna Saint-Ange for editing the manuscript and Ms Christine Gaillard for secretarial assistance.

References

1. Yousem DM. Dashed hopes for MR imaging of the head and neck: the power of the needle. *Radiology* 1992;184:25–26
2. Gussack GS, Hudgins PA. Imaging modalities in recurrent head and neck tumors. *Laryngoscope* 1991;101:119–124
3. Teresi LM, Lufkin RB, Hanafee WN. Magnetic resonance imaging of the larynx. *Radiol Clin North Am* 1989;27:393–406
4. Bonnerot V, Charpentier A, Frouin F, Kalifa C, Vanel D, Di Paola R. Factor analysis of dynamic magnetic resonance imaging in predicting the response of osteosarcoma to chemotherapy. *Invest Radiol* 1992;27:847–855
5. Bazin JP, Di Paola R, Gibaud B, Rougier P, Tubiana M. Factor analysis of dynamic scintigraphic data as a modelling method: an application to the detection of metastases. In: Di Paola R, Kahn E, eds. *Information Processing in Medical Imaging*. Paris: INSERM, 1979:345–366
6. Di Paola R, Bazin JP, Aubry F, et al. Handling of dynamic sequences in nuclear medicine. *IEEE Trans Nucl Sci* 1982;29:1310–1321
7. UICC. *TNM Classification of Malignant Tumors*. 4th ed. Berlin: Springer-Verlag, 1987:3–4
8. Som PM, Shapiro MD, Biller HF, Sasaki C, Lawson W. Sinonasal tumors and inflammatory tissues: differentiation with MR imaging. *Radiology* 1988;167:803–808
9. Sigal R, Monnet O, De Baere T, et al. Adenoid cystic carcinoma of the head and neck: evaluation with MR imaging and clinical-pathologic correlation in 27 patients. *Radiology* 1992;184:95–101
10. Sulfaro S, Frustaci S, Volpe R, et al. A pathologic assessment of tumor residue and stromal changes after intraarterial chemotherapy for head and neck carcinomas. *Cancer* 1989;64:994–1001
11. Lee JKT, Glazer HS. Contreversy in the MR imaging appearance of fibrosis. *Radiology* 1990;177:21–22
12. Erlemann R, Sciuk J, Bosse A, et al. Response of osteosarcoma and Ewing sarcoma to preoperative chemotherapy: assessment with dynamic and static MR imaging and skeletal scintigraphy. *Radiology* 1990;175:791–796
13. Nyman RS, Rehn SM, Glimelius BLG, Hagberg HE, Hemmingsson AL, Sundström CJ. Residual mediastinal masses in Hodgkin disease: prediction of size with MR imaging. *Radiology* 1989;170:435–440
14. Barber DC. The use of the principal components in the quantitative analysis of gamma camera dynamic studies. *Phys Med Biol* 1980;25:283–292
15. Frouin F, Bazin JP, Di Paola M, Jolivet O, Di Paola R. FAMIS: A software package for functional feature extraction from biomedical multidimensional images. *Comput Med Imaging Graph* 1992;16:81–91
16. Kaissar G, Kim JH, Bravo S, Sze G. Histologic basis for increased extraocular muscle enhancement in gadolinium-enhanced MR imaging. *Radiology* 1991;179:541–542
17. Watson AD, Rocklage SM, Carvlin MJ. Contrast agents. In: Stark DD, Bradley WG Jr, eds. *Magnetic Resonance Imaging*. 2nd ed. Saint-Louis: Mosby, 1992:379–381
18. Gammill SL, Shipkey FH, Himmelfarb EH, Parvey LS, Rabinowitz JG. Roentgenology-pathology correlative study of neovascularity. *AJR Am J Roentgenol* 1976;126:376–385
19. Viamonte M, Roen S, LePage J. Nonspecificity of abnormal vascularity in angiographic diagnosis of malignant neoplasms. *Radiology* 1973;106:56–63
20. Dock W, Grabenwöger F, Metz V, Eibenberger K, Farrés MT. Tumor vascularization: assessment with duplex sonography. *Radiology* 1991;181:241–244
21. Michaels L. *Ear, Nose and Throat Histopathology*. Heidelberg: Springer-Verlag, 1987:133
22. Johnson GK, Squier CA, Johnson WT, Todd GL. Blood flow and epithelial thickness in different regions of feline oral mucosa and skin. *J Oral Pathol* 1987;16:317–321
23. Allard M, Doucet D, Kien P, Bonnemain B, Caillé JM. Experimental study of DOTA-Gadolinium: pharmacokinetics and pharmacologic properties. *Invest Radiol* 1988;23(suppl 1):271–274
24. Bousquet JC, Saini S, Stark DD, et al. Gd-DOTA: characterization of a new paramagnetic complex. *Radiology* 1988;166:693–698